Effect of Thymoquinone on Skeletal Muscle Innervation in Induced Degeneration of the Hamster Buccal Pouch

Asmaa MF Abd El-Wahed[1], Ahmed MM Korraah[2], Fadia MAttia [3], Magda MA Hassan[4].

[1]Assistant lecturer in Oral Pathology, M.D, Faculty of Dentistry, Kilo 6 Ring Road, Suez Canal University, Ismailia, Egypt. E-mail:(asmaa_elwahed@dent.suez.edu.eg, dentistasmaa87@yahoo.com). +2 01111307770. The corresponding author.
2 Lecturer of Oral Pathology, PhD, Faculty of Dentistry, Suez Canal University, Ismailia, Egypt.
3 Professor of Clinical Pathology, Head of Clinical Pathology Department, Faculty of Medicine, Suez Canal University, Ismailia, Egypt.
4 Professor of Oral Pathology, Faculty of dentistry, Suez Canal University, Ismailia, Egypt.

Abstract: Aim of the study: *This research aimed to study the effect of TQ on skeletal muscle innervation in the 7, 12-dimethylbenz[a]anthracene (DMBA) - induced degeneration of the hamster buccal pouch (HBP).* ***Material and Methods:*** *70 male golden Syrian hamsters were divided into 3 groups. Group A: (5) untreated animals (negative control group). Group B: (5) animals, topically treated with 0.5% 7,12-dimethylbenz[a]anthracene (DMBA) 3/week/6weeks (positive control group). Group C: (60) animals were treated as group B, then divided equally into two sub-groups CI and CII. They received one and two i.p thymoquinone (TQ) (0.1 mg/kg body weight) injection(s), respectively, then 5 animals from each subgroup were euthanized at 1, 2, 4, 7, 14, and 20 days after the last TQ injection(s).All HBPs were surgically excised, fixed and processed for H&E, immunohistochemistry (IHC) staining of neurofilament heavy chain (NFH) and quantitative real time polymerase chain reaction technique (RT-PCR) for detection of muscle specific tyrosine kinase (MuSk). The obtained data were statistically analysed.****Results:*** *The left buccal pouches in group B were markedly shortened and nearly restored their length after TQ treatment. The muscle fibres (MFs) were progressively forming from 7 and 4 days after one and two TQ injection(s), respectively. The NFH stain intensity were progressively increasing after TQ treatment as focal MFs membranes' plaques. The MuSk expression was downregulated in group B. After TQ injection(s), its expression slightly increased during MFs proliferation, and markedly expressed at differentiation and fusion stages of MFs.* ***Conclusion:*** *TQ stimulates re-innervation of skeletal muscles in HBPs.*

Keywords:*7,12-dimethylbenz[a]anthracene.Thymoquinone. Neurofilament heavy chain. Neuromuscular junction. Muscle specific tyrosine kinase.*

I.   Introduction

Skeletal muscles comprise large percentage of the human body mass and play very important role in locomotion, postural support, and breathing[1]. Many stimuli / conditions can cause their injury as: (a) muscle dystrophy; (b) exposure to myotoxic agents, such as cardio toxin or lidocaine; (c) sharp or blunt trauma, such as punctures or contusions, (d) ischemia, (e) exposure to hot or cold temperatures, and (f) the muscle's own contraction [2].

After muscle fibers' injury, they regenerate and restore damaged myofibers [3]. Muscle regeneration occurs in five interrelated and time-dependent phases, namely, degeneration (necrosis), inflammation, regeneration, remodeling, and maturation/ functional repair [2]. Innervation of skeletal muscle fibers (MFs) is essential for maintenance of muscle size, structure, and function [4]. The newly formed neuromuscular junction (NMJs) between the surviving neurons' axons and regenerated MFs can be noted within two weeks of muscle injury [5]. The initial phases of muscle regeneration do not depend on neural influence, but the subsequent growth and maturation require presence of the nerve. The presence of nerve can directly influence protein turnover and gene expression within multinucleated regenerating myotubes and indirectly influence the proliferation and differentiation of satellite cells [3].

Skeletal muscle fibers are innervated by large, myelinated motor neurons originating from the anterior horn of the spinal cord. The end of each motor axon has 20–100 thin unmyelinated terminal branches, each

---

innervates a single muscle fiber. The NMJ is the key functional unit that controls muscle contraction. They are assembled on the muscle fibers at very precise locations called end plates (EP) [6].

Nicotinic acetylcholine receptor (nAChR) cauterizes at the end plates. As soon as the action potential reaches the axon terminals, it induces opening of the voltage-gated Ca2+ channels influx on the presynaptic nerve membrane. In turn this allows Ca2+ influx to induce synaptic vesicles fusion with the presynaptic membrane then releasing the neurotransmitter nACh in the synaptic cleft. Then, nACh diffuses and binds to nAChRs localized on the postsynaptic membrane of the muscle fibre [7].This binding makes nAChRs permeable to both Na+ and K+, i.e. opens the associated voltage-gated Na+ channels on the muscle membrane, initiating an action potential causing Ca2+ release from the sarcoplasmic reticulum into the cytosol, then muscle contraction [8].Acetylcholinesterase (AchE) located on the synaptic portion of the basal lamina (that envelops muscle fibres), quickly inactivates the released nAChs and neurotransmission stops [9]. Unfortunately, any stimulus could impair this complex process of signal transmission, causing muscle weakness or paralysis, and affect the quality of life[7].

Many genes are required for synaptogenesis include Muscle-specific tyrosine kinase (MuSK),downstream-of-tyrosine-kinase-7 (Dok-7), low-density lipoprotein receptor-related protein (Lrp4), neuronal Agrin and rapsyn [10]. MuSkis a single transmembrane receptor involved in all aspects of NMJ development. The low-density lipoprotein receptor-related protein 4 (Lrp4-MuSK) receptor complex is necessary for triggering postsynaptic differentiation upon binding to neural agrin[11].Dok-7 is a downstream adaptor protein to Musk that is important for activation of MuSk and maintaining the structural integrity of the endplate [10].

Neurofilaments (NFs) are intermediate filaments (IF) with a diameter of 10 nm. They are present in dendrites, perikarya (i.e. the cell body of a neuron), and abundant in axons. They are essential for the radial growth of axons during development, maintenance of axon caliber and transmission of electrical impulses along axons, i.e. velocity of nerve conduction [12]. After neurofilaments synthesis in the perikarya, they are quickly translocated into the axons and assemble into filamentous structures [13]. NFs are composed of three subunits, defined by their molecular weight: NF-L (light chain), NF-M (medium chain) and NF-H (heavy chain), weighing 60 kilodalton (kDa), 100 kDa and 110 kDa, respectively [14]. The three NF subunits are expressed at distinct stages of vertebrate development, triggered by neuron differentiation [15].

Taken together, injured peripheral nerves and skeletal muscles have a remarkable ability for tissue regeneration, where functional NMJs occurs after injury [16].

The 7, 12-dimethylbenz [a]-anthracene (DMB) is one member of the polycyclic aromatic hydrocarbons (PAHs) that present in cigarette smoke. It has cytotoxic, carcinogenic, mutagenic and immunosuppressive effects [17]. DMBA has been widely used to induce carcinogenesis in rodent oral cancer (OC) models specially hamster buccal pouches (HBPs) [18].

Thymoquinone (TQ) the major active constituent of Nigella sativa Linnaeus (NS. L), is one of the promising medicinal plants [19]. TQ has neuroprotective effects through antioxidant and anti-inflammatory activities. It also prevent neuroinflammation by inhibiting inflammatory mediators as NO, prostaglandin E2 (PGE2), TNF-α, and IL-1β production in microglial cells [20]. It was found that TQ prevents muscle and nerve tissues' damage during Dewley rat's ischemia-reperfusion (IR) of a lower limb [21].

In HBP/DMBA model, the few DMBA paintings resulted in necrosis of the pouches ' distal end with shortening of their length to about 2cm. These painted pouches do not regain their full length even after cessation of DMBA painting. Elongation of these pouches with regeneration of striated muscle fibers under the effect of different TQ preparations and concentrations was reported in previous studies carried out in the present lab[22-24].

II. Material And Methods
Approval of the Research Ethical Committee (REC), Faculty of Dentistry, Suez Canal University has been obtained before starting the search (approval number is 265/2020).
II.1Animals
The present study was carried out on 70 male golden Syrian hamsters (Mesocrietus auratus) purchased from the Holding Company for Biological Products and Vaccines (VACERA), Helwan, Cairo, Egypt. They were about 100-120 grams. Hamsters were kept five per cage in a well-ventilated room with controlled temperature, 50-70 % humidity and 12 hours day/night cycle, in the Animal House, Faculty of Dentistry, Suez Canal University. They were given water and recommended diet ad libitum.
II.2 Chemicals and reagents
II.2.1Carcinogen
One gram of DMBA (cat. no: D3254) dissolved in 200 ml of heavy mineral oil (cat.No: M 3516) to get 0.5% solution. Both were purchased from Sigma Chemical Company, St. Louis, Mo, USA. using a magnetic stirrer. It was topically applied to the left HBPs using number 4 camel hairbrushes.

II.2.2Thymoquinone (TQ)

TQ solution (0.1 ml/L) was prepared by dissolving 1 gm of TQ in 100 ml propylene glycol (to get a 0.1 mg/kg body weight) using a magnetic stirrer, until getting a homogenous (clear) solution. TQ was purchased from Sigma Chemical Company, Saint Louis, Mo, USA.

II.2.3The kit of NFH IHC stain

NFH rabbit monoclonal antibodies, (Cat. No: A19084) was purchased from ABclonal technology, 500W Cummings Park, Ste. 6500 Woburn, Massachusetts 01801, USA. The used dilution was 1:100. The stain was detected using Ultravision detection system (Cat. No. TP-015-HD).

II.2.4RT-PCR kits

The real time polymerase chain reaction technique (RT-PCR) was used. The snap frozen fresh sections of HBPs were homogenized in Biozol reagent (Invitrogen, Carlsbad, CA, USA). The RNA extraction was performed simply using total RNA extraction kit (Cat. No. BSC52S1, Bio-Flux, China) according to the manufacturer's instructions. Then, RNA was reverse transcribed. Quantitative real-time PCR was carried out with an ABI 7300 Sequence Detection System (Applied Biosystems, Foster City, CA, USA) using SYBR green.

II.3 The experimental design:

The 70 hamsters were divided into 3 groups. Group A: (5) untreated animals, served as negative control and were euthanized at day zero. Group B: (5 animals) their left pouches were painted with DMBA (3/week/6weeks), served as positive control and euthanized at second day of last painting. Group C: the experimental group (60 animals) treated as group B, then were divided equally into two sub-groups as follow: Group CI: received one i.p. injection with TQ (0.1 mg/kg body weight). Whereas Group CII: received two i.p. injections with TQ (0.1 mg/kg body weight) day after day. 5 animals from each subgroup were euthanized at 1, 2, 4, 7, 14, and 20 days after the last TQ injection(s).

The euthanization was done by inhalation of a lethal dose of ether (soaked cotton piece with ether and kept in a tightly-closed glass container). Then all pouches were surgically excised, a thin slice from each pouch was cut and frozen for quantitative real time polymerase chain reaction (RT-qPCR). The rest of the pouches were fixed in 10% neutral puffer formalin and embedded in soft paraffin wax, 5μm sections were cut, processed for H&E and immunohistochemical (IHC) stain for light microscope study.

II.4Histopathologic evaluation

Grading of epithelial dysplasia (OED) was done according to Bánóczy and Csiba [25] into: mild dysplasia: when an average of less than 3 dysplastic criteria were present, moderate dysplasia: when an average of 3-7 criteria were present, severe dysplasia: when an average of 7 or more criteria were present, and carcinoma in situ (CIS): when all or some of the dysplastic criteria were distributed from top to bottom with intact basement membrane.

II.5Immunohistochemical analysis

The indirect technique (avidin–biotin complex) (ABC) was used. The slides were diagnosed by two pathologists and photographed by Olympus E-330 Evolt Digital Photography camera using Image Analyzing System (Olympus BX50 Microscope). Semi-quantitative method was used to determine the immunohistochemical stain intensity using the recent version of ImageJ software with IHC profiler plugin (1.48 version) (NIH, Bethesda, Maryland) (Java 1.8.9_66).

The final score was shown in semi-quantitative way (high positive, positive, low positive or negative). The scores were classified into four categories: negative =0, low positive =1, positive =2 and high positive =3 according to the stain intensity [26]. The mean of NFH stain intensity was determined by using the semi-quantitative IHC protocol [27].

II.6Quantitative real time polymerase chain Reaction (RT-qPCR)

The muscle-specific tyrosine kinase (MuSK) gene expression was evaluated via quantitative real time polymerase chain Reaction (RT-qPCR). Fresh specimen from both pouches of all groups were snap frozen and stored at −80 °C. then homogenized in in Biozol reagent (Invitrogen, Carlsbad, CA, USA). Total RNA was extracted according to the manufacturer's instructions. After RNA extraction, cDNA was synthesized immediately. RNA was reverse transcribed using first strand cDNA kit (Cat.No. K1622, Fermentas, USA) according to manufacturer's instructions. Then, the cDNA was amplified by using SYBR green. cDNA samples were diluted tenfold before introducing into qPCR reaction. Relative expression was determined by comparison to the 'house-keeping' gene, Glyceraldehyde-3-phosphate dehydrogenase (GAPDH), using the geNorm software (v3.5). The primer sets used for PCR analysis were MuSK-F "TGAGAACTGCCCCTTGGAACT", MuSK-R "GGGTCTATCAGCAGGCAGCTT", GAPDH-F "CGTGTTCCTACCCCCAATGT", and GAPDH-R "TGTCATCATACTTGGCAGGTTTCT".

The thermal cycling profile consists of 95 °C for 4 min followed by 40 cycles of denaturation at 95 °C for 30 s, annealing at 60 °C for 30 s and elongation at 72 °C for 18 s.The mean values of quantitation cycle (Cq) is the number of cycles needed for amplification to reach a specific threshold level of detection. Delta Cq value was calculated by subtracting the geometric mean of validated reference gene from the raw Cq value of the MuSK gene. Delta deltaCq value yields a normalized relative gene expression value. It was calculated by normalization

of a gene target with experimental treatment to the reference gene whose expression remain unchanged by the treatment. Subsequently, this value was normalized to the targeted gene expression detected in the control sample.

II.7Statistical analysis

The mean of IHC stain intensity and relative MuSK gene expression normalized ratios for all groups were expressed as mean ± standard deviation and statistically analyzed using ANOVA test by the software Statistical Package for Social Sciences (SPSS) (version 12.0). The mean difference is significant at $p \leq 0.05$ level.

III. Result

III.1 Clinical observations: The animals of group A (the negative control) appeared healthy with normal appearing pouches (clear and whitish in color) that measured about 5-6 cm. Whereas animals of group B showed,perioral hair loss of their left side and the left HBPs were severely inflamed with ulcers and exophytic masses and necrosis at the distal ends. They also showed marked shortening of their left pouches to about 2 cm **(Figure 1 and 2)**. After one and two TQ injection(s) and by the end of experiment, the left pouches measured about 4.5-5 cm.

III.2 Histopathological evaluation: The HBPs of group A, showed normal mucosa of both sides **(Figure 3A)**. Whereas group B showed degenerated distal end with severe dysplastic epithelium with focal superficial invasion. The bulk of muscle layer was markedly reduced **(Figure 3B)**. On the other hand,at 7 and 4 days after one and two TQ injection(s), respectively, the surface epithelium showed moderate to mild dysplasia with thinner and slightly inflamed lamina propria. The muscle layer bulk was progressively forming. At 20 days after TQ injection(s),the surface epithelium appeared normal with near normal thickness of muscle layer**(Figures4)**.

III.3 The NFH immunohistochemical assessment:The intensity of IHC stain was moderate as seen at the MFs membranes 'plaquesin group A.While in group B, the some MFs membranes' plaquesshowed mild stain. After one and two TQ injection(s), in all experimental groups,the intensity of NFH IHC stain was progressively increasing from 2 and 1 day(s) to 20 days **(Figure 5)**.

III.4 TheRT-qPCRof MuSK gene expression: Transcripts of MuSK gene was slightly higher in negative control group where mean Cq normalization values were = 1 ± 0, while in positive control group the mean normalized Cq values were = 0.28 ± 0.083. The MuSK gene gradually increased in the experimental groups till reaching near its expression level of group A at 7 and 4 days after one and two TQ injection(s), respectively. i.e. mean Cq normalized values were = 1 ± 0.8 and 1 ± 0. Then, the gene continued its increase till the end of experiment.

III.5 Statistical analysis of mean IHC stain intensity and mean expression of MuSK gene:The mean difference of IHC stain intensity and relative MuSK gene expression between subgroups was significant at p value of ≤ 0.05. The stain intensity of NFH was significantly decreased in group B (positive control group) when compared with group A (negative control group). The intensity of NFH started to increase gradually after TQ treatment in both groups CI and CII. It reached the peak at 20 days after one and two TQ injection(s), respectively **(Table 1 and 2)**.Whereas MuSKof both group A and group B showed no statistically significant differences when compared with CI at (1, 2, 4, 7, and 14 day(s) after one TQ injection) subgroups and CII at (1, 2, 4 and 7 day(s) after two TQ injections) subgroups. While MuSKshowed statistically significant differences between both group A and group B when compared to CI at 20 days after one TQ injection subgroup and CII at 14 and 20 days after two TQ injections subgroups at $p\leq0.05$**(Table 3 and 4)**.
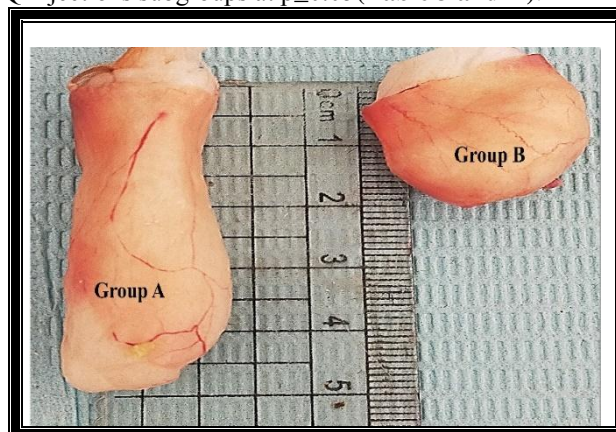
Figure 1: Gross presentation of buccal pouches of groups A and B. The pouch of hamsters from group A (negative control) measuring about 5 cm, while marked shortening of the left pouch from group B (positive control), measuring about 2 cm.
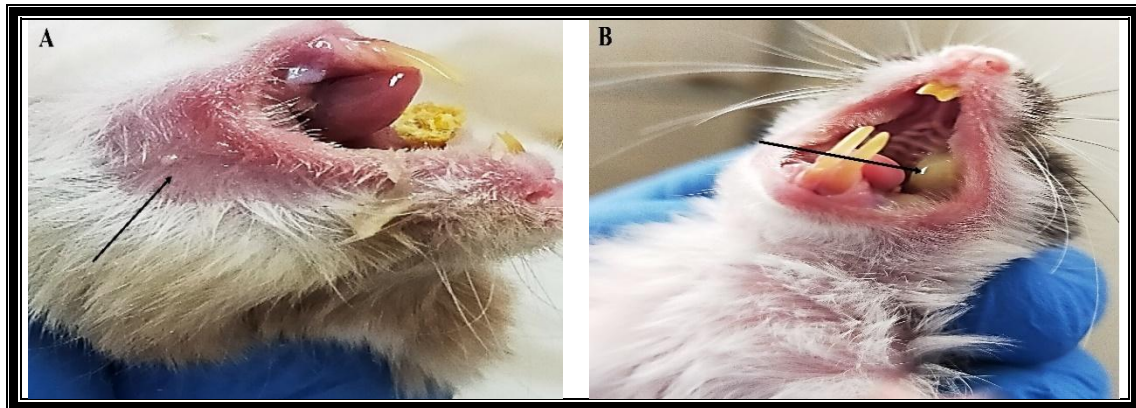
Figure 2: Clinical appearance of group B (positive control) (DMBA 3/week/6weeks). A: The left side of hamsters' cheek showing perioral hair loss. B: severe inflammation with necrotic mass of the left pouch (arrow).
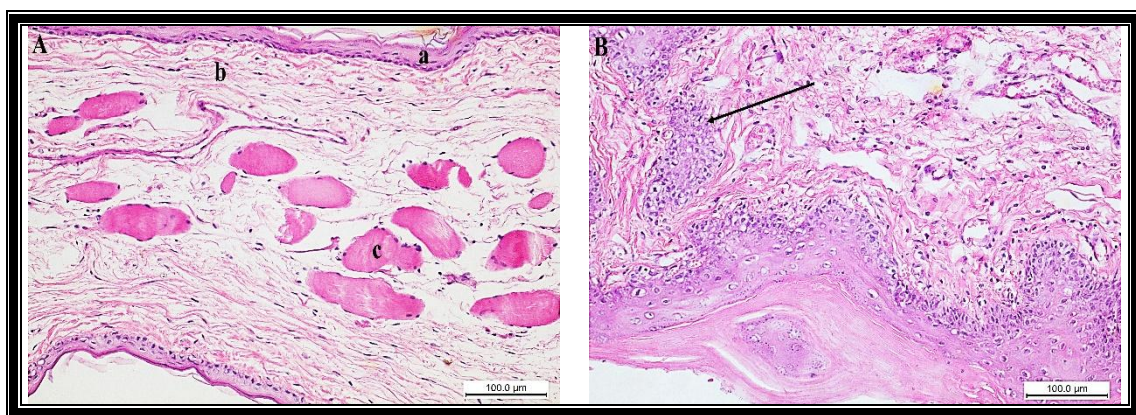
Figure 3: Photomicrographs of left buccal pouches from negative and positive control groups. (A) Showing normal buccal pouch formed of thin keratinized epithelium (a), non-inflamed thin lamina propria (b), and loose muscle fibers(c). (B) Near the distal end of left pouches, the epithelial lining showed hyperplastic, dysplastic epithelium with superficial invading islands (arrow) with no MFs (A and B: H&E).
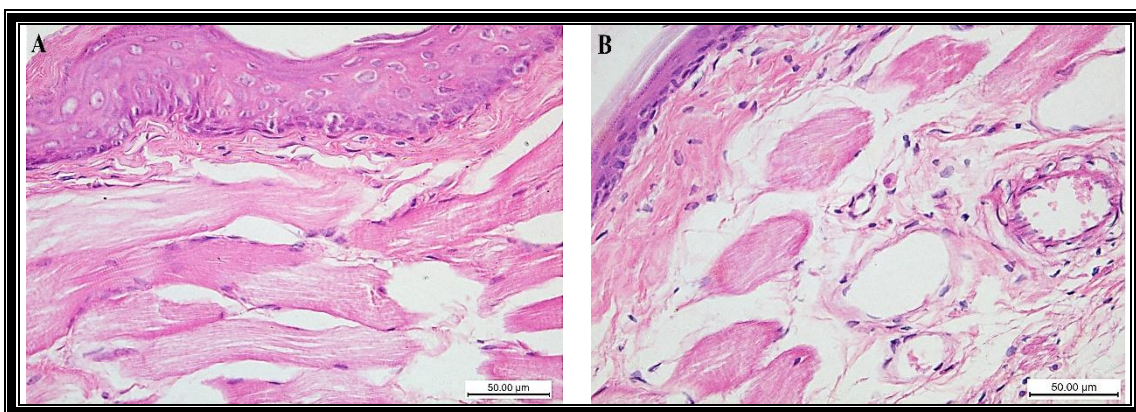
Figure 4: Photomicrographs of left pouches after TQ treatment. (A) Showing peripherally located nuclei of increased MFs, at 4 days after TQ treatment. (B) Showing the thickness of loose muscle layer bulk to near normal, at 20 days after TQ treatment (A&B: H&E).
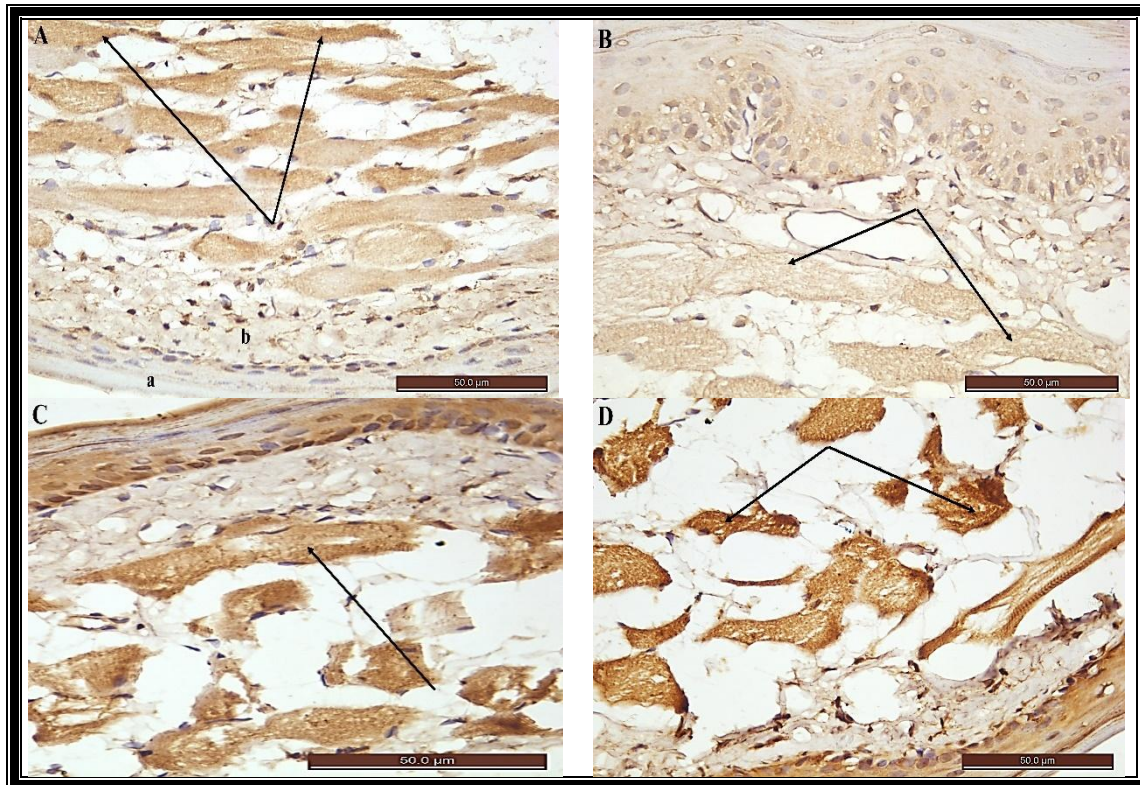
Figure 5: Photomicrographs of NFH immunohistochemistry-stained sections of left buccal pouches. (A): Showing negative stain of epithelial cells (a), moderate stain of lamina propria fibroblasts (b), and moderate diffuse stain of muscle fibers with focal MFs'membranous plaques (arrows) in negative control group. (B) Showing mild diffuse stain of MFs' (arrows) in positive control group. (C) Showing increasing NFH IHC stain intensity of MFs and their membranes' plaques (arrows) at 20 days after one TQ injection. (D): Showing increased NFH stain intensity membranes' plaques (arrows) at 20 days after two TQ injections (A, B, C, and D: NFH ABC-DAB).

Table 1: Results of NFH immunohistochemical stain intensity of all CI subgroups, compared to both group A and group B.

Groups	Mean ± standard deviation	Significance at different times of euthanization							
		G A	G B	1 day	2 days	4 Days	7 Days	14 days	20 days
Group A	121±4.9		.00*	.00*	.00*	.00*	1	.12	.01*
Group B	77.4±3.37	.00*		.00*	.00*	.00*	.00*	.00*	.00*
CI (1 day)	86.8±3.8	.00*	.00*		.01*	.00*	.00*	.00*	.00*
CI (2 days)	93.9±3.9	.00*	.00*	.01*		.00*	.00*	.00*	.00*
CI (4 days)	107.9±3.3	.00*	.00*	.00*	.00*		.00*	.00*	.00*
CI (7 days)	120.9±2.04	1	.00*	.00*	.00*	.00*		.09	.01*
CI (14 days)	126.2±1.4	.12	.00*	.00*	.00*	.00*	.09		.99
CI (20 days)	127.8±1.5	.01*	.00*	.00*	.00*	.00*	.01*	.99	

(*) The mean difference was significant at $p \leq 0.05$.

Table 2: Results of NFH immunohistochemical stain intensity of all CII subgroups, compared to both group A and group B.

Groups	Mean ± standard deviation	Significance at different times of euthanization							
		G A	G B	1 day	2 days	4 days	7 days	14 days	20 days
Group A	121±4.9		.00*	.00*	.00*	.95	.76	.00*	.00*
Group B	77.4±3.37	.00*		.00*	.00*	.00*	.00*	.00*	.00*
CII (1 day)	94.6±4.6	.00*	.00*		.00*	.00*	.00*	.00*	.00*
CII (2 days)	109.8±2.1	.00*	.00*	.00*		.00*	.00*	.00*	.00*
CII (4 days)	118.9±1.78	.95	.00*	.00*	.00*		.09	.00*	.00*
CII (7 days)	124±1.76	.76	.00*	.00*	.00*	.09		.29	.00*
CII (14 days)	128.2±1.12	.00*	.00*	.00*	.00*	.00*	.29		.03*
CII (20 days)	134±1.9	.00*	.00*	.00*	.00*	.00*	.00*	.03*	

(*) The mean difference was significant at p≤0.05.

Table 3: Results of RT-qPCR of MuSK gene expression of all CI subgroups, compared to both group A and group B.

Groups	Mean ± standard deviation	Significance at different times of euthanization							
		G A	G B	1day	2 days	4days	7 days	14 days	20 days
Group A	1±0		.20	.72	.85	1.0	1.0	1.0	.00*
Group B	0.28±0.083	.20		.99	.98	.48	.20	.15	.00*
CI (1 day)	0.52±0.08	.72	.99		1.0	.95	.72	.63	.00*
CI (2 days)	0.58±0.08	.85	.98	1.0		.99	.85	.77	.00*
CI (4 days)	0.86±0.15	1.0	.48	.95	.99		1.0	.99	.00*
CI (7 days)	1±0.8	1.0	.20	.72	.85	1.0		1.0	.00*
CI (14 days)	1.04±0.89	1.0	.15	.63	.77	.99	1.0		.00*
CI (20 days)	3.8±0.44	.00*	.00*	.00*	.00*	.00*	.00*	.00*	

(*) The mean difference was significant at p≤0.05

Table 4: Results of RT-qPCR of MuSK gene expression of all CII subgroups, compared to both group A and group B.

Groups	Mean ± standard deviation	Significant at different times of euthanization							
		G A	G B	1 day	2 days	4 days	7 days	14 days	20 days
Group A	1±0		.41	.98	.99	1.0	1.0	.00*	.00*
Group B	0.28±0.08	.41		.98	.94	.41	.27	.00*	.00*
CII (1 day)	0.64±0.08	.98	.98		1.0	.98	.92	.00*	.00*
CII (2 days)	0.70±0.07	.99	.94	1.0		.99	.97	.00*	.00*
CII (4 days)	1±0	1.0	.41	.98	.99		1.0	.00*	.00*
CII (7 days)	1.08±0.8	1.0	.27	.92	.97	1.0		.00*	.00*
CII (14 days)	2.8±0.8	.00*	.00*	.00*	.00*	.00*	.00*		.00*
CII (20 days)	4.8±0.8	.00*	.00*	.00*	.00*	.00*	.00*	.00*	

(*) The mean difference was significant at p≤0.05.

IV. Discussion

The Syrian golden hamster has features that nearly resemble the main physiologic and metabolic activities of humans [17]. The 0.5% concentration of DMBA was found to be capable of inducing severe dysplasia in the HBPs after 6 to 8 weeks of painting [18].In previous studies, the early few DMBA paintings result in

necrosis of the distal pouch, with reduction of its length due to degenerated buccal pouches' muscles (from bout 5-6 cm to about 2cm) These shortened pouches did not regain the full length even after DMBA painting cessation [23, 28, 29].

Moreover, DMBA induces marked inflammation of HBPs. In a previous study, the serum tumor necrosis factor- α (TNF-α), i.e.one of the inflammatory mediators, showed statistically significant elevation after topical application due to its systemic toxic effect [24]. Furthermore, topical DMBA can increase lipid peroxidation and reactive oxygen species (ROS) which cause structural nerve damage and mediate the carcinogenic process by inducing chronic inflammatory state and mutations[30].

This study used very low concentration of TQ, for its powerful anti-inflammatory and antioxidant effects at low concentrations [30, 31]. Furthermore, TQ has many neuroprotective effects with inhibition of lipid peroxidation-inflammatory mediators' production [30, 32]. The present study investigated the effect of small dose of TQ on innervation of regenerating skeletal muscle fibers, of the hamster buccal pouches(HBPs), after being degenerated by painting DMBA. In a previous study that used the same TQ concentration at the same time with DMBA painting for 6 weeks, showed that the DMBA-painted pouches were elongated to near normal length with healed necrosis, mild inflammatory infiltrate and prevention of epithelial malignancy progression [22].

This work followed the time sequence of the classic muscle regeneration rout, as reported by Chargé and Rudnicki (2004), Musarò (2014), and Forcina *et al*, (2020). In classic way, muscle regeneration occurs in 5 interrelated and time-dependent phases. After injection of cardiotoxin (CTX) in mice or rats plantaris', soleus' or tibialis' muscles, it produces a local myonecrosis. After few hours of CTX treatment, neutrophils infiltrate between the necrotic tissue and this necrotic phase extends up to 2 days. The inflammatory phase started after 2-3 hours of CTX injection and extend up to 4 days. After 2 days, spindle-shaped mononucleated cells mixed with necrotic debris, leukocytes, and macrophages appear. The regeneration phase started 2 days after CTX treatment and extends up to 14 days. By 7–10 days after CTX injection, most of muscle bulk was restored. These regenerated MFs are smaller with centrally located myonuclei. The progressive maturation of regenerating myofibers was reported to occur 10 to 15. While the innervation and functional restoration was reported from 15-20 days after CTX injection [2, 3, 33].

In an ongoing work, muscle regeneration showed different timing of each phase than that of the classic route of muscle regeneration. Timing of each phase was reported to depend on the type of organism (e.g., mouse, rat, and human), type of muscle, the extent of damage, and the animal model used [3, 33]. This work and the ongoing one used different animal model and different muscle type, as HBPs' muscles considered free end muscle.

The animals of group A (negative control) were healthy and active, with normal appearing left and right pouches that measured about 5-6 cm. Whereas animals from group B showed perioral hair loss, inflammed left pouches with multiple ulcers, and exophytic mases with marked shortening of left pouches' length to about 2 cm **(Figures 1 and 2)**. The muscle layer bulk showed marked reduction in group B compared to group A **(Figure 3)**, while it was progressively forming from 7 and 4 days after one and two TQ injection(s), respectively, and reached to near normal thickness at about 20 days after one and two TQ injection(s). The pouches measured about 4.5-5.5 cm, with no ulceration or inflammation and complete healing of distal ends necrosis. These results were comparable to findings of previous studies **(Figure 4)**[22, 23, 28, 29].

In group B, at the distal end, the new formed MFs were multinucleated, i.e. mostly developed through activation of satellite cells of injured MFs (the classic regeneration route)[2].On the other hand, at all time intervals, the new MFs, in the TQ-treated animals, were mature (peripherally located nuclei), possibly formed by other stem cells as reported by previous studies used comparable protocols[22-24].These studies reported Myo-D positive mononuclear perivascular cells, fibroblasts of the lamina propria, and FAP cells at the distal end. The authors proposed that the increased muscle bulk was gained by myogenic differentiation of these cells.

In an ongoing work, by this group, PAX-7 IHC positive cells were the same cells reported by the aforementioned studies. All these studies did not investigate the innervation and functional maturation of the new MFs.

The present study used the NFH IHC stain as a marker of peripheral motor nerve alteration during the experiment as used in study of Tu *et al*, (2017) [34].In group A, the NFH showed moderate stain intensity of MFs membranes' plaques. These findings supported the normal functions of NFs as members of the cytoskeleton proteins that act together to form and maintain cell shape and facilitate the transport of particles and organelles within the cytoplasm [35]. In group B, the muscle fibers (MFs) showed mild NFH stain.Stirling and Stys (2010), explained these findings as after peripheral nerve injuries, the nerve axon distal to injury site, remain intact for some days before granular disintegration of the cytoskeleton [36].

Group A showed statistically significant difference when compared with group B (positive control), both CI at (1-, 2-, 4-, and 20-day(s)) **(Table 1)** and CII at (1-, 2-, 14- and 20-day(s)) subgroups **(Table 2)**. Group B showed statistically significant differences when compared with groups A, and all C subgroups **(Tables 1 and 2)**.

After 1 day of one TQ injection the NFH showed mild stain of focal MFs membranes 'plaques. These findings were a response of nerve injury and the state of inflammation as reported in previous studies [37, 38]. Moreover, these findings may be due to the delayed phosphorylation and subsequent axon transport. As the phosphorylation of NFM and NFH were found to be delayed until newly formed NF assemblies have translocated into axons [39]. The presence of positive focal membranous' plaques after one day of one TQ injection, could also be explained due to axons regeneration where NF subunits reemerge in a temporal sequence reminiscent of that in developing neurons [40].

The intensity of NFH stain was increasing from day 2 to 20 days after one and two TQ injection(s), respectively **(Figure 5)(Tables 1, 2)**. This can be explained due to the progressive healing of nerves, as reported by Faussone-Pellegrini et al. (1999), Yuan et al. (2017) and Zhao and Szaro, (1995) [40-42]. Furthermore, these findings indicated the cumulative effect of TQ injection(s).

Muscle specific tyrosine kinase (MuSK) is involved in the formation, maintenance and integrity of the neuromuscular junction (NMJ). Disruption of MuSK protein expression can cause pronounced disassembly of the entire NMJ [11]. Moreover, Richman *et al*. (2012), found that animals immunized with anti-MuSK developed severe progressive muscle weakness, weight loss, muscle endplate destruction and abnormal nerve terminals [43]. Furthermore, any mutations that impair MuSK activity, cause congenital myasthenia gravis characterized by structurally and functionally defective synapses, leading to muscle weakness and fatigue [44].

The MuSK expression was reported to remain up-regulated during muscle development, then dramatically down-regulated in mature muscle, where it remains prominent only at the NMJ, i.e. partially involved in early muscle development and essential for the function of NMJ in mature MFs [45, 46]. Moreover, MuSK expression was found to be re-induced throughout the myofibers following denervation, block of electrical activity, and physical immobilization, this suggested the roles of MuSK in response to injury, atrophy, or changes in muscle activity [45].

In the present work, MuSK expression in group A was slightly higher than that in group B, with the mean Cq normalization values were = 1 ± 0 in group A, while the mean normalized Cq values were = 0.28 ± 0.083 in group B. This reduced expression was not statistically significant. These findings were consistent with Bryant et al, (2017), who reported that after injury of gastrocnemius skeletal muscle, the post-synapse revealed down regulation of NMJ genes such as MuSK and Rapsyn [47]. Moreover, these findings were contradictory to Valenzuela et al. (1995), who reported MuSK protein is dramatically induced by denervation as is MuSK mRNA. They further reported that MuSK protein induction was apparent 2 days after denervation and reached maximum levels at 2 weeks. These contradicting results may be due to difference of nerve injury induction. In the present study, DMBA induced nerve injury and degeneration, while in Valenzuela *et al*. (1995) study, complete denervation was done by nerve cuts and crushes. Or could be due to different animal models (hamsters' pouch in the present work vs rats' embryonic muscle cells in Valenzuela *et al*[45].

The expression of MuSK in the present work was gradually increased during MFs proliferation (1, 2 and 4 days after one TQ injection) and (1 and 2 days after two TQ injections) then its expression reached the base line level (as the negative control group) at 7 and 14 days after one injection, or 4 and 7 days after two TQ injections, i.e., at end of myoblast proliferation and differentiation. During nerve crush injury that allowed to re-innervate, MuSK protein levels were found to return to baseline [45, 46]. This slight increase showed no statistically significant differences when compared to groups A and B **(Tables 3, 4)**.

The expression of MuSK was markedly increased with significant difference at 20 days after one TQ injection and at 14, and 20 days after two TQ injections compared to groups A and B, i.e., during MFs differentiation and maturation.[3, 33] The results further support the cumulative effect of two TQ injections.

V. Conclusion

Nerve regeneration in this model follows MFs regeneration, as shown by NFH expression that was decreased after DMBA application due to nerve and muscle necrosis. Then, gradually increased during development till reaching threshold level, at which the expression declines possibly due to dephosphorylation and subsequent proteasomal degradation. Moreover, neuromuscular junction (NMJ) formation, maturation and preservation was in parallel to the muscle specific tyrosine kinase (MuSK) gene expression. MuSK is expressed at low levels at early MFs formation and up regulated during their differentiation stage, while dramatically downregulated in mature muscle, where it remains prominent only at the NMJ.

References

[1] Juhas M, Bursac N. Engineering skeletal muscle repair. Current Opinion in Biotechnology. 2013; 24: 880-886. https://doi.org/10.1016/j.copbio.2013.04.013.

[2] Chargé SB, Rudnicki MA. Cellular and molecular regulation of muscle regeneration. Physiology Reviews. 2004; 84: 209-238. https://doi.org/10.1152/physrev.00019.2003.

[3] Forcina L, Cosentino M, Musarò A. Mechanisms regulating muscle regeneration: Insights into the interrelated and time-dependent phases of tissue healing. Cells. 2020; 9: 1297-1325. https://doi.org/10.3390/cells9051297.

[4] Beehler BC, Sleph PG, Benmassaoud L, Grover GJ. Reduction of skeletal muscle atrophy by a proteasome inhibitor in a rat model of denervation. Experimental biology and medicine 2006; 231: 335-341. https://doi.org/10.1177/153537020623100315.

[5] Rizzuto E, Pisu S, Nicoletti C, Del Prete Z, Musarò A. Measuring neuromuscular junction functionality. Journal of Visualized Experiments. 2017; 126: 1-9. https://doi.org/10.3791/55227.

[6] Arrowsmith JE. The neuromuscular junction. Surgery (Oxford). 2007; 25: 105-111. https://doi.org/10.1016/j.mpsur.2007.02.001.

[7] Ferraro E, Molinari F, Berghella L. Molecular control of neuromuscular junction development. Journal of Cachexia, Sarcopenia and Muscle. 2012; 3: 13-23. https://doi.org/10.1007/s13539-011-0041-7.

[8] Wu H, Xiong WC, Mei L. To build a synapse: signaling pathways in neuromuscular junction assembly. Development. 2010; 137: 1017-1033. https://doi.org/10.1242/dev.038711.

[9] Colquhoun D, Sakmann B. Fast events in single- channel currents activated by acetylcholine and its analogues at the frog muscle end- plate. Journal of Physiology. 1985; 369: 501-557. https://do.org/10.1113/jphysiol.1985.sp015912.

[10] Okada K, Inoue A, Okada M, Murata Y, Kakuta S, Jigami T, Kubo S, Shiraishi H, Eguchi K, Motomura M. The muscle protein Dok-7 is essential for neuromuscular synaptogenesis. Science. 2006; 312: 1802-1805. https://doi.org/10.1126/science.1127142.

[11] Hesser BA, Henschel O, Witzemann V. Synapse disassembly and formation of new synapses in postnatal muscle upon conditional inactivation of MuSK. Molecular and cellular neurosciences. 2006; 31: 470-480. https://doi.org/10.1016/j.mcn.2005.10.020.

[12] Yum SW, Zhang J, Mo K, Li J, Scherer SS. A novel recessive *NEFL* mutation causes a severe, early- onset axonal neuropathy. Annals of Neurology. 2009; 66: 759-770. https://doi.org/10.1002/ana.21728.

[13] Liu Y, Guo Y, Xu L, Wu S, Wu D, Yang C, Zhang Y, Li C. Alternation of neurofilaments in immune-mediated injury of spinal cord motor neurons. Spinal Cord. 2009; 47: 166-170. https://doi.org/10.1038/sc.2008.90.

[14] Yan Y, Jensen K, Brown A. The polypeptide composition of moving and stationary neurofilaments in cultured sympathetic neurons. Cell Motility and the Cytoskeleton. 2007; 64: 299-309. https://doi.org/10.1002/cm.20184.

[15] Yan Y, Brown A. Neurofilament polymer transport in axons. The Journal of Neuroscience. 2005; 25: 7014-7021. https://doi.org/10.1523/JNEUROSCI.

[16] Darabid H, Perez-Gonzalez AP, Robitaille R. Neuromuscular synaptogenesis: coordinating partners with multiple functions. Nature Review Neuroscience. 2014; 15: 703-718. https://doi.org/10.1038/nrn3821.

[17] Cekanova M, Rathore K. Animal models and therapeutic molecular targets of cancer: utility and limitations. Drug Design, Development and Therapy. 2014; 2014: 1911-1922. https://doi.org/10.2147/DDDT.S49584.

[18] Shklar G. Development of experimental oral carcinogenesis and its impact on current oral cancer resecuch. Journal of Dental Research. 1999; 78: 1768-1772. https://doi.org/10.1177/00220345990780120101.

[19] Woo C, Kumar A, Sethi G, Tan K. Thymoquinone: potential cure for inflammatory disorders and cancer. Biochemical Pharmacology. 2012; 83: 443-451. https://doi.org/10.1016/j.bcp.2011.09.029.

[20] Wang Y, Gao H, Zhang W, Zhang W, Fang L. Thymoquinone inhibits lipopolysaccharide-induced inflammatory mediators in BV2 microglial cells. International Immunopharmacology. 2015; 26: 169-173. https://doi.org/10.1016/j.intimp.2015.03.013.

[21] Erkut A, Cure M, Kalkan Y, Balik M, Guvercin Y, Yaprak E, Yuce S, Sehitoglu I, Cure E. Protective effects of thymoquinone and alpha-tocopherol on the sciatic nerve and femoral muscle due to lower limb ischemia-reperfusion injury. European Review for Medical and Pharmacological Sciences. 2016; 20: 1192-1202.

[22] Algharyni HM, El-Hossary WH, Korraah AM, Hassan MM. Expression of MyoD in the DMBA-treated hamster pouches following thymoquinone injection. IOSR Journal of Dental and Medical Sciences (IOSR-JDMS). 2019; 18: 35-40. https://doi.org/10.9790/0853-1802043540

[23] Hassan M, Abdel-Latif G, El-Hossary W. Protective and promising myogenic effect of two thymoquinone formulations in relation to the pouch-induced carcinogenic model. IOSR Journal of Dental and Medical Sciences (IOSR-JDMS). 2017; 16: 54-66. https://dOI.org/10.9790/0853-1605035466.

[24] Hassan M, El-Hossary W, Hanafi R. Anti-inflammatory thymoquinone and muscle regeneration in the hamster buccal pouch-induced dysplasia. Journal of Oral Health and Dental Science. 2020; 4: 302.

[25] Bánóczy J, Csiba Á. Occurrence of epithelial dysplasia in oral leukoplakia: analysis and follow-up study of 12 cases. Oral surgery, oral medicine, and oral pathology. 1976; 42: 766-774. https://doi.org/10.1016/0030-4220(76)90099-2.

[26] Mane DR, Kale AD, Belaldavar C. Validation of immunoexpression of tenascin-C in oral precancerous and cancerous tissues using ImageJ analysis with novel immunohistochemistry profiler plugin: An immunohistochemical quantitative analysis. Journal of Oral and Maxillofacial Pathology 2017; 21: 211-217. https://doi.org/10.4103/jomfp.JOMFP_234_16.

[27] Crowe A, Yue W. Semi-quantitative determination of protein expression using Immunohistochemistry staining and analysis: An integrated protocol. Bio Protocol. 2019; 9: e3465-e3476. https://doi.org/10.21769/BioProtoc.3465.

[28] Elmansy M, Shata MS, El Borady O. Effect of nano-thymoquinone on tumor necrosis factor-α in DMBA-induced hamster buccal pouch carcinogenesis. Egyptian Dental Journal. 2020; 66: 2389-2400. https://doi.org/10.21608/edj.2020.41942.1246.

[29] El-Sherbiny RH, Hassan MM, Korraah AM. Effect of different nanothymoquinone concentrations on the chemically-induced epithelial dysplasia in the hamster buccal pouch. Suez Canal University of Medicine Journal. 2017; 20: 75-88. https://doi.org/10.21608/scumj.2017.46990.

[30] Hassanein KM, El-Amir YO, Practice. Protective effects of thymoquinone and avenanthramides on titanium dioxide nanoparticles induced toxicity in Sprague-Dawley rats. Pathology Research and Practice. 2017; 213: 13-22. https://doi.org/10.1016/j.prp.2016.08.002.

[31] Das S, Dey KK, Dey G, Pal I, Majumder A, MaitiChoudhury S, kundu SC, Mandal M. Antineoplastic and apoptotic potential of traditional medicines thymoquinone and diosgenin in squamous cell carcinoma. Public Library of Science one (PLoS One). 2012; 7: e46641. https://doi.org/10.1371/journal.pone.0046641.

[32] Anbalagan V, Raju K, Shanmugam M. Assessment of lipid peroxidation and antioxidant status in vanillic acid treated 7,12-dimethylbenz[a]anthracene Induced hamster buccal pouch carcinogenesis. Journal of Clinical and Diagnostic Research : JCDR. 2017; 11: BF01-BF04. https://doi.org/10.7860/JCDR/2017/23537.9369.

[33] Musarò A. The Basis of Muscle Regeneration. Advances in Biology. 2014; 2014: 1-16. https://doi.org/10.1155/2014/612471.

[34] Tu H, Zhang D, Corrick RM, Muelleman RL, Wadman MC, Li YL. Morphological Regeneration and Functional Recovery of Neuromuscular Junctions after Tourniquet-Induced Injuries in Mouse Hindlimb. Front Physiol. 2017; 8: 1-9. 10.3389/fphys.2017.00207.

[35] Liu Q, Xie F, Siedlak S, Nunomura A, Honda K, Moreira PI, Zhua X, Smith M, Perry G. Neurofilament proteins in neurodegenerative diseases. Cellular and Molecular Life Sciences : CMLS. 2004; 61: 3057-3075. https://doi.org/10.1007/s00018-004-4268-8.

[36] Stirling D, Stys P. Mechanisms of axonal injury: internodal nanocomplexes and calcium deregulation. Trends in Molecular Medicine. 2010; 16: 160-170. https://doi.org/10.1016/j.molmed.2010.02.002.

[37] Hoffman P, Pollock S, Striph G. Altered gene expression after optic nerve transection: reduced neurofilament expression as a general response to axonal injury. Experimental, Neurology. 1993; 119: 32-36. https://doi.org/10.1006/exnr.1993.1004.

[38] Yuan A, Sasaki T, Rao MV, Kumar A, Kanumuri V, Dunlop DS, Liem RK, Nixon RA. Neurofilaments form a highly stable stationary cytoskeleton after reaching a critical level in axons. J Neurosci. 2009; 29: 11316-11329. https://doi.org/10.1523/JNEUROSCI.1942-09.2009

[39] Nixon RA, Paskevich PA, Sihag RK, Thayer CY. Phosphorylation on carboxyl terminus domains of neurofilament proteins in retinal ganglion cell neurons in vivo: influences on regional neurofilament accumulation, interneurofilament spacing, and axon caliber. J Cell Biol. 1994; 126: 1031-1046. https://doi.org/10.1083/jcb.126.4.1031.

[40] Zhao Y, Szaro B. The optic tract and tectal ablation influence the composition of neurofilaments in regenerating optic axons of Xenopus laevis. The Journal of Neuroscience. 1995; 15: 4629-4640. https://doi.org/10.1523/JNEUROSCI.15-06-04629.1995

[41] Faussone-Pellegrini M-S, Matini P, DeFelici M. The cytoskeleton of the myenteric neurons during murine embryonic life. Anatomy and embryology. 1999; 199: 459-469. https://doi.org/10.1007/s004290050244.

[42] Yuan A, Rao M, Veeranna R, Nixon R. Neurofilaments and Neurofilament Proteins in Health and Disease. Cold Spring Harbor Perspectives in Biology. 2017; 9: a018309. https://do.org/10.1101/cshperspect.a018309.

[43] Richman DP, Nishi K, Morell SW, Chang JM, Ferns MJ, Wollmann RL, Maselli RA, Schnier J, Agius MA. Acute severe animal model of anti-muscle-specific kinase myasthenia: combined postsynaptic and presynaptic changes. Archives of neurology. 2012; 69: 453-460. https://doi.org/10.1001/archneurol.2011.2200.

[44] Burden SJ, Yumoto N, Zhang W. The role of MuSK in synapse formation and neuromuscular disease. Cold Spring Harbor perspectives in biology. 2013; 5: a009167-a009167. https://doi.org/10.1101/cshperspect.a009167.

[45] Valenzuela DM, Stitt TN, DiStefano PS, Rojas E, Mattsson K, Compton DL, Nunez L, Park JS, Stark JL, Gies DR. Receptor tyrosine kinase specific for the skeletal muscle lineage: expression in embryonic muscle, at the neuromuscular junction, and after injury. Neuron. 1995; 15: 573-584. https://doi.org/10.1016/0896-6273(95)90146-9.

[46] Yilmaz A, Kattamuri C, Ozdeslik R, Schmiedel C, Mentzer S, Schorl C, Oancea E, Thompson T, Fallon J. MuSK is a BMP co-receptor that shapes BMP responses and calcium signaling in muscle cells. Science Signaling. 2016; 9: ra87. https://doi.org/10.1126/scisignal.aaf0890.

[47] Bryant J, MacKrell J, Gifondorwa D, Yaden B, Monroe B, Tyler K, Davis J, Culver A, Shetler P, Jadhav P. Molecular changes at the post-synapse and improved motor function suggest accelerated recovery with SARM treatment in an androgen-depleted animal model of nerve injury. Journal of Musculoskeletal-Disorders andTreatment. 2017; 3: 1-10. https://doi.org/10.23937/2572-3243.1510037.